Experimental and theoretical approach to spin splitting in modulation-doped $In_xGa_{1-x}As/InP$ quantum wells for $B \rightarrow 0$

G. Engels, J. Lange, Th. Schäpers, and H. Lüth
Institut für Schicht- und Ionentechnik, Forschungszentrum Jülich GmbH, 52425 Jülich, Germany
(Received 26 August 1996)

Spin splitting of conduction-band energy levels in a modulation-doped $InP/In_{0.77}Ga_{0.23}As/InP$ quantum well has been studied by Shubnikov–de Haas oscillations. By analyzing the characteristic beating pattern of the oscillations the coupling constant α for spin-orbit interaction was determined. Biasing a gate on top of a Hall bar was used to modify the strength of the spin-orbit coupling. The measured spin-orbit coupling parameter α is quantitatively explained by utilizing a refined envelope-function-approximation theory for heterostructures. [S0163-1829(97)51704-8]

At zero or low magnetic fields, conduction-band electrons in III-V heterostructures are usually treated as spin degenerated. Depending on the symmetry of the heterostructure it can occur that spin-orbit coupling leads to a splitting into two-spin separated levels. In the past, different theoretical models were developed in order to describe the origin of the spin splitting. One explanation is based on the fact that the zinc-blende lattice of common III-V semiconductors, e.g., GaAs, is asymmetric with respect to inversion.[1,2] This bulk crystal contribution leads to a spin split proportional to k^3. In addition, spin-orbit coupling can also be induced by a surface electric field of a heterostructure, the so-called Rashba term.[3,4] Here, the electric field due to band bending in a two-dimensional electron gas (2DEG) or in an asymmetric quantum well couples to the spin of the electrons in the conductive channel. Theoretically, it was shown that narrow gap semiconductors, such as InSb or InAs, exhibit a strong Rashba-like behavior, whereas the k^3 dependence is dominant in wide gap materials such as $Al_xGa_{1-x}As/GaAs$.[5–7]

Experimentally, spin split III-V heterostructures can be studied by measuring Shubnikov–de Haas (SdH) oscillations. A characteristic beating pattern indicates the occupation of two different subbands due to spin-orbit coupling of the electrons in the channel. Using this method, the spin-orbit coupling of electrons in a GaSb/InAs/GaSb quantum well was measured by Luo *et al.*[8,9] By comparing samples with different quantum-well widths it was concluded that the Rashba term is the dominant spin-splitting mechanism for the specific quantum well and that the k^3 term can be neglected. Lifting of the spin degeneracy was also studied on strained $In_xGa_{1-x}As/In_{0.52}Al_{0.48}As$ quantum wells.[10,11] Here, it was shown that the Rashba spin-orbit term dominates over the bulk k^3term. A comparison of the theoretically estimated spin-splitting energy with the experimentally determined value only showed poor agreement. The experimental value exceeded the calculated one by a factor of ≈ 2.6.[11]

In order to get further insight into the spin-splitting mechanisms, we performed Shubnikov–de Haas studies on gate-controlled strained $InP/In_{0.77}Ga_{0.23}As/InP$ quantum wells. By applying a gate voltage on a metallic gate covering the Hall bar structure the symmetry of the underlying quantum well was varied systematically. The spin-orbit coupling parameter as a function of the gate voltage was determined from the measured beating pattern in the Shubnikov–de Haas oscillations. A detailed analysis of the Rashba term shows that the simple approach, by only calculating the contribution of the expectation value of the electric field inside the quantum well, is not sufficient to get a good agreement between theory and experiment. As has already been observed by Das *et al.*,[11] the theoretically obtained spin-orbit coupling parameter is, in this case, much smaller than the experimentally deduced α. By using a refined envelope-function theory, a very good agreement between theory and experimental values was obtained.

We have used a heterostructure grown by metal organic vapor phase epitaxy on a semi-insulating InP $\langle 100 \rangle$ substrate. First, a 500-nm-thick InP buffer layer was grown followed by a 10-nm-thick, 1.0×10^{18} cm^{-3} n-doped InP layer, and a 8-nm-thick InP spacer layer. Subsequently, a 10-nm-thick strained $In_{0.77}Ga_{0.23}As$ channel layer was grown which was finally capped by a 40-nm-thick undoped InP layer. By using a quantum well, which is only 40 nm below the surface, the potential profile of the well can easily be modified by biasing a gate on top of the layer system. A 200-μm-wide and 600-μm-long Hall bar was prepared by wet chemical mesa etching. Ohmic contacts of Ni/AuGe/Ni (5 nm/90 nm/25 nm) were tempered at 400 °C for 2 min. Finally, a layer of 150-nm-thick PECVD-SiO_2 (plasma-enhanced chemical-vapor deposition) was deposited followed by a Cr/Au gate structure (5 nm/100 nm) covering the electrically active region of the Hall bar completely. The fully prepared sample yields a carrier concentration of $n = 1.59 \times 10^{12}$ cm^{-2} and a mobility of $\mu = 200\,500$ $cm^2/V\,s$ at zero-voltage gate bias.

The SdH oscillations shown in Fig. 1. are measured in lock-in technique with a current of 1 μA at a temperature of 0.3 K. The gate voltage is applied between the 2DEG and the top metallization layer. The voltage was adjusted between -6 and $+2$ V without any measurable leakage current through the SiO_2 insulation layer. For positive voltages higher than $+2$ V, the SdH pattern does not change significantly. The carrier concentration in the channel saturates without filling the second subband. For a voltage below -6 V the SdH-oscillations vanish between 0 and 1.2 T. The spin-orbit coupling parameter thus can not be extracted.

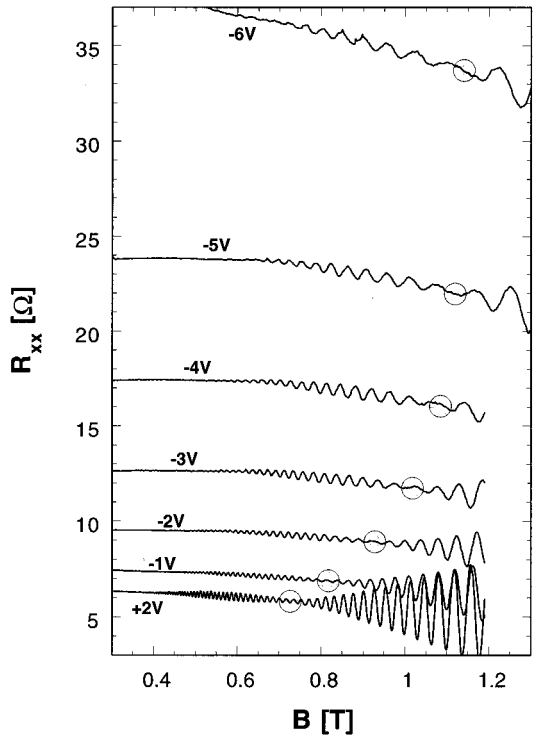

FIG. 1. Shubnikov–de Haas oscillations at a temperature of 0.3 K with the gate voltage changed as a parameter.

There are three major features clearly resolved. First, the carrier concentration is lowered due to negative gate voltages. This can be seen by the diminished SdH frequency (Fig. 2). Second, as a consequence of the reduction of carrier density and the reduced mobility, the resistance at $B=0$ increases. Third, the position of the nodes in the SdH amplitude is shifted which indicates a change in the beating effect between two closely spaced SdH frequencies.

The $1/B$ Fourier transform of the longitudinal magnetoresistance, shown in Fig. 2, clearly resolves a double-peak structure. The (horizontal) frequency axis is normalized to spin degeneracy as is typically done for SdH evaluation of the two-dimensional carrier concentration. When more than one frequency peak appears for a given SdH measurement, one has to take the sum of the corresponding carrier concentrations. This is correct for multiple peaks originating from the occupation of multiple two-dimensional subbands. The sum of the carriers typically yield the carrier concentration of standard Hall-effect measurements. In our case, the sum of the carriers taken from the double-peak structure is exactly twice as high as the Hall concentration indicating that we have to deal with a single two-dimensional subband split into two nonspin-degenerate sublevels. The density of states $Z_{\pm}(E)$ as a function of electron energy of each spin subband is therefore half the density of a degenerated two-dimensional subband $Z=m^*/(\pi\hbar^2)$ modified by an energy-dependent correction factor

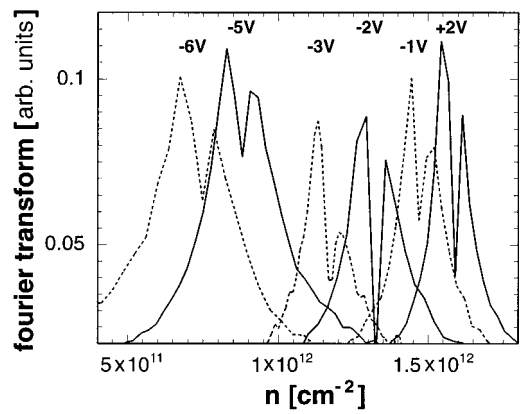

FIG. 2. Fourier transform taken from the SdH oscillations of Fig. 1.

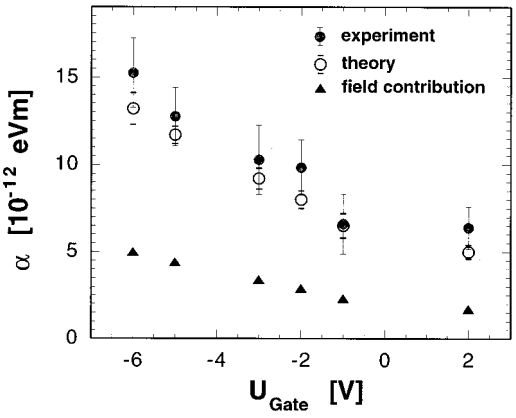

FIG. 3. Values for the spin-orbit coupling parameter α given by experiment and theory. The error bars of the experimental values result from the finite width of the peaks in the Fourier spectra, while the error bars of the theoretical values result from the numerical errors resulting from the determination of the electron wave function.

$$Z_{\pm}(E)=\frac{1}{2}\frac{m^*}{\pi\hbar^2}\left(1\mp\frac{1}{\sqrt{1+(2E\hbar^2)/(\alpha^2 m^*)}}\right).$$

This expression is derived from the energy eigenvalues ε of an unperturbated two-dimensional subband with Rashba spin-orbit coupling:

$$E=E^{\mathrm{sub}}+\frac{\hbar^2\underline{k}_{\|}^2}{2m^*}\pm|\underline{k}_{\|}|.$$

α is the spin-orbit coupling coefficient, E^{sub} is the energy of the ith two-dimensional subband, E is the energy above the subband bottom, m^* is the direction-independent effective mass in the conducting channel, and $\underline{k}_{\|}$ is the electron wave vector in the two-dimensional layer.

By taking the differences in carrier concentration Δn of the spin subbands at low temperature and low magnetic fields ($B<1.5$ T) from the Fourier spectra in Fig. 2, we use

$$\Delta n=n_- - n_+=\int_0^{E_F} Z_-(E)dE-\int_0^{E_F} Z_+(E)dE$$

$$\Rightarrow\alpha=\frac{\Delta n\hbar^2}{m^*}\sqrt{\frac{\pi}{2(n-\Delta n)}}$$

for the computational of the experimental values of the spin-orbit coupling parameter α (Fig. 3).[13] It is seen that α mo-

notonously increases from an initial value of 6.3×10^{-12} eV m for a gate voltage of $+2$ V up to a maximum value of 15.3×10^{-12} eV m at -6 V. As confirmed by the following theoretical calculation of α, biasing the gate with a more negative voltage leads to an increase of the net electric field in the well and consequently to an increase of the Rashba spin-orbit term.

Our theoretical calculation of the coupling constant α is based on an improved envelope-function theory.[12] Usually the envelope-function theory is used for the description of electronic bulk semiconductor states, where the electronic states are described by the product of a band-edge Bloch function and an envelope function. Since the envelope function only changes in large distances in comparison with the lattice constant, this method is known to be limited to slowly varying potentials. For the calculation of α, an improved envelope-function theory was developed which can deal with abrupt potential changes as they occur in heterostructures. Since the k^3 contribution can be neglected for our material system,[11] only the Rashba term was considered. Within this new framework the expression for the spin-orbit coupling parameter α of our particular quantum well is given by

$$\alpha = \frac{\hbar^2 E_p}{6 m_0}\{a'\langle \mathcal{E}_A\rangle + b'(\langle \mathcal{E}_{B_u}\rangle + \langle \mathcal{E}_{B_l}\rangle) - \tfrac{1}{2} b(|\Psi_u|^2 - |\Psi_l|^2)\},$$

where E_p is the $\mathbf{k}\cdot\mathbf{p}$ interaction parameter. The value $E_p = 22$ eV used here for our $In_{0.53}Ga_{0.47}As$ channel material was linearly interpolated from the values of InAs and GaAs. $\langle \mathcal{E}_A\rangle$ is the expectation value of the electric field in the channel (A), whereas $\langle \mathcal{E}_{B_u}\rangle$ and $\langle \mathcal{E}_{B_l}\rangle$ are the expectation values in the upper and lower InP barriers (B_u, B_l), respectively. $|\Psi_u|^2$ and $|\Psi_l|^2$ are the squared electron probabilities at the upper and lower conduction band discontinuities, respectively. The prefactors a', b', and b are given by

$$a' = \left(\frac{1}{(E - E_{\Gamma_7}^{(A)})^2} - \frac{1}{(E - E_{\Gamma_8}^{(A)})^2} \right),$$

$$b' = \left(\frac{1}{(E - E_{\Gamma_7}^{(A)} - \Delta E_{\Gamma_7})^2} - \frac{1}{(E - E_{\Gamma_8}^{(A)} - \Delta E_{\Gamma_8})^2} \right),$$

$$b = \left(\frac{\Delta E_{\Gamma_7}}{(E - E_{\Gamma_7}^{(A)} - \Delta E_{\Gamma_7})^2} + \frac{\Delta E_{\Gamma_7}}{(E - E_{\Gamma_7}^{(A)})^2} - \frac{\Delta E_{\Gamma_8}}{(E - E_{\Gamma_8}^{(A)} - \Delta E_{\Gamma_8})^2} - \frac{\Delta E_{\Gamma_8}}{(E - E_{\Gamma_8}^{(A)})^2} \right).$$

Here, E is the energy of the electronic state in the quantum well. From the expressions for a', b', and b it can be seen that the Γ_6 conduction band of the channel layer is coupled to the energetic nearest neighbors, in our case the Γ_7 and Γ_8 valence band maxima. For $b'$and b, the differences ΔE_{Γ_7} and ΔE_{Γ_8} between the Γ_7 and Γ_8 band of the channel material (A) and the barrier material (B) has to be considered in addition. Since $E_{\Gamma_7}^{(A)}$ and $E_{\Gamma_8}^{(A)}$ is of the order of eV, while the energetic distance between E and $E_{\Gamma_6}^{(A)}$ is usually of the order of meV, we neglect $E - E_{\Gamma_6}^{(A)}$ for the computation of α.

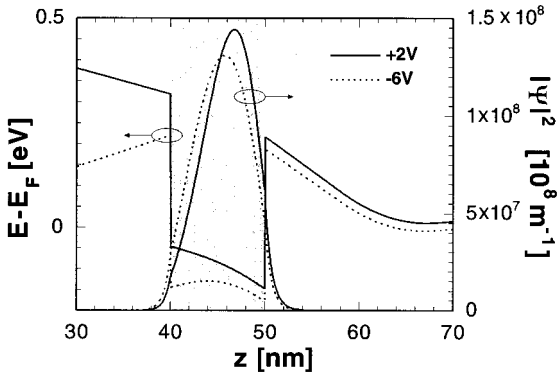

FIG. 4. Conduction-band potential and electron probability for a gate voltage of $+2$ V (full line) and -6 V (dashed line).

The contribution $a'\langle \mathcal{E}_A\rangle$ describes the spin-orbit coupling originating from the quantum well alone. If a quantum well with infinite potential barriers is assumed, this would be the only contributions to the Rashba spin-orbit coupling term. Indeed, the $a'\langle \mathcal{E}_A\rangle$ term is, in principle, identical to the Rashba term derived by de Andrada e Silva *et al.*,[7] for a triangular well with an infinite potential barrier at the interface. For a finite barrier, as in our case, the electron wave function leaks into the barrier, which results in an additional contribution $b'(\langle \mathcal{E}_{B_u}\rangle + \langle \mathcal{E}_{B_l}\rangle)$. Finally, the abrupt change of the potential at the heterointerfaces leads to a term which is proportional to the difference of the electron probability at the heterointerfaces. This contribution would vanish only in the case when the electron probability is identical on both sides of the quantum well.

By using a self-consistent Schrödinger-Poisson solver,[14] we computed the particular potential profile of the conduction band, the electron wave function $\Psi(z)$, and the electric field $\mathcal{E}(z) = -d\phi(z)/dz$ as a function of growth direction z necessary for the determination of the theoretical value of α. The variation of the gate voltage on top of the sample is

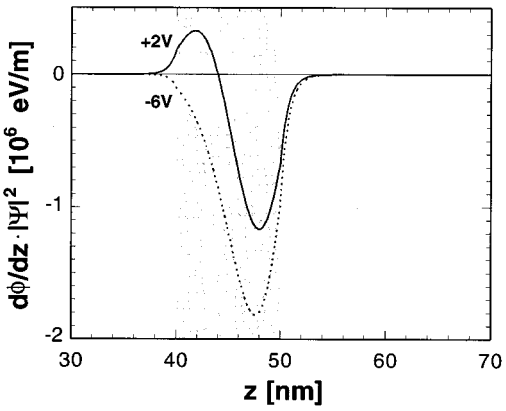

FIG. 5. Electric field weighted by the electron probability for a gate voltage of $+2$ V (full line) and -6 V (dashed line).

introduced to the numerical simulation by varying the surface pinning of the conduction band in each computation in order to fit the particular experimental sheet carrier concentration. The conduction band profiles for gate voltages of -6 V and $+2$ V are shown in Fig. 4 together with the corresponding electron wave functions. The electric field weighted by the electron probability density is shown in Fig. 5. One can clearly resolve the very strong change in spatial symmetry due to the applied voltage at the surface of the sample which alters the spin coupling. The nearly rectangular shaped potential at $V_{\text{gate}}=+2$ V is much more symmetric with respect to its center ($z=45$ nm) than the triangle formed conduction band for $V_{\text{gate}}=-6$ V. As a consequence, the electron probability density is shifted away from the middle yielding a larger difference at the channel boundaries. Thus the theoretical values for α in Fig. 3 clearly rise for negative gate voltages which fits the experimental findings quantitatively, very well. In addition, the pure field-induced contribution to α in the channel material is also plotted, since it clarifies the importance of the derived interface probability terms for the calculation of α. For a gate bias of $+2$ V the electric field changes sign within the quantum well (Fig. 4). Consequently, this leads to a smaller value of the $a'\ \langle \mathcal{E}_A \rangle$ contribution to α in comparison to the -6 V gate bias.

In conclusion, the Rashba spin-orbit coupling of the conduction-band electrons in InP/In_xGa_{1-x}As/InP quantum-well structures was investigated. By covering a Hall bar with a gate, it was possible to change the symmetry of the quantum well in a defined fashion by applying an external gate voltage. The corresponding spin-orbit coupling constant could be extracted from the characteristic beating pattern of the Shubnikov–de Haas oscillations. A comparison with the results of a refined envelope-function theory shows that the contribution of the electric field in the quantum well does not explain the strength of the measured spin-orbit coupling alone. Quantitative agreement between experiment and theory is obtained by including additional interface terms together with electric-field-induced coupling inside the barrier.

The authors would like to thank M. Hollfelder and H. Hardtdegen for the growth of the InP/In_xGa_{1-x}As/InP heterostructure, A. Leuther for using his Schödinger-Poisson solver, and G. Müllejans for his excellent assistance during the measurements.

[1] G. Dresselhaus, Phys. Rev. **100**, 580 (1955).
[2] M. Cardona, N. E. Christensen, and G. Fasol, Phys. Rev. B **38**, 1806 (1989).
[3] E. I. Rashba, Fiz. Tverd. Tela (Leningrad) **2**, 1224 (1960).
[4] Y. A. Bychokov and E. I. Rashba, J. Phys. C **17**, 6039 (1984).
[5] U. Rössler, F. Malcher, and G. Lommer, Phys. Rev. Lett. **60**, 728 (1988).
[6] U. Rössler, F. Malcher, and G. Lommer, in *Solid State Science*, edited by G. Landwehr (Springer, Berlin, 1989), Vol. 87, p. 376.
[7] E. A. de Andrada e Silva, G. C. La Rocca, and F. Bassani, Phys. Rev. B **50**, 8523 (1994).
[8] J. Luo, H. Munekata, F. F. Fang, and P. J. Stiles, Phys. Rev. B **38**, 10 142 (1988).
[9] J. Luo, H. Munekata, F. F. Fang, and P. J. Stiles, Phys. Rev. B **41**, 7685 (1990).
[10] B. Das, D. C. Miller, S. Datta, R. Reifenberger, W. P. Hong, P. K. Bhattacharya, J. Singh, and M. Jaffe, Phys. Rev. B **39**, 1411 (1989).
[11] B. Das, S. Datta, and R. Reifenberger, Phys. Rev. B **41**, 8278 (1990).
[12] J. Lange (unpublished).
[13] The small contribution below zero energy of Z_- was neglected in the intergration for n_-.
[14] A. Leuther, Ph.D. thesis, RWTH-Aachen, Germany, 1996.